Energy transmission in a mechanically-linked double-wall structure coupled to an acoustic enclosure

L. Cheng,[a] Y. Y. Li, and J. X. Gao
Department of Mechanical Engineering, The Hong Kong Polytechnic University, Hung Hom, Kowloon, Hong Kong SAR, China

(Received 3 May 2004; revised 14 February 2005; accepted 16 February 2005)

The energy transmission in a mechanically linked double-wall structure into an acoustic enclosure is studied in this paper. Based on a fully coupled vibro-acoustic formulation, focus is put on investigating the effect of the air gap and mechanical links between the two panels on the energy transmission and noise insulation properties of such structures. An approximate formula reflecting the gap effect on the lower-order coupled frequencies of the system is proposed. A criterion, based on the ratio between the aerostatic stiffness of the gap cavity and the stiffness of the link, is proposed to predict the dominant transmitting path, with a view to provide guidelines for the design of appropriate control strategies. Numerical results reveal the existence of three distinct zones, within which energy transmission takes place following different mechanisms and transmitting paths. Corresponding effects on noise insulation properties of the double-wall structure are also investigated. © *2005 Acoustical Society of America.* [DOI: 10.1121/1.1886525]

PACS numbers: 43.20.Tb, 43.40.At [MO] Pages: 2742–2751

I. INTRODUCTION

Double-wall structures are widely used in noise control engineering due to their superiority over single-leaf structures in providing better acoustic insulation. Typical examples include vehicles, partition walls in buildings and aircraft fuselage shells, etc. Early work can be traced back to London,[1] who discussed the sound transmission through double-leaf panels using a simplified model consisting of two identical walls. The model was then extended by Beranek,[2] leading to the London–Beranek model for noise transmission analysis of double walls with identical mass. Since then, the topic has received a great deal of attention. Various numerical techniques, such as the statistical energy analysis and the finite element approach, have been used for transmission calculation.[3–5]

A clear understanding of the energy transmission mechanism between the two panels is of paramount importance in the design of such structures. Among other parameters, the air gap separating the two walls plays a critical role. A practical method for estimating the sound transmission loss of double walls was presented by Iwashige and Ohta[6] and was applied to analyze the popular case of light panels with an air gap. Antonio *et al.*[7] observed that the influence of the air gap on sound reduction was frequency dependent. At low frequencies a better performance was achieved using a thicker air layer, while at higher frequencies a thinner air layer was preferable. Meanwhile, filling the gap with porous sound absorbing materials to increase the sound insulation capability of such structures has also been investigated.

Double-wall structures, however, are less efficient at low frequency around the mass–air–mass resonance at which the model for infinite panels reveals an out-of-phase motion of the two walls.[8] Until quite recently, there has been a persistent effort to explore the potential of using active controls to increase the transmission loss of double-wall partitions at low frequencies.[9–14] Literature review shows that most previous studies used structures without any mechanical connections between the two walls. In such cases, sound/vibration energy is entirely transmitted through the air gap, i.e., from the acoustic transmitting path. In many applications, however, there exist mechanical links to connect the two walls. As a result, energy might also be transmitted from the link, thus forming the structural transmitting path. In this regard, Bouhioui investigated the effect of mechanical joints on double wall systems using the finite element method.[15] Bao and Pan experimentally examined the effect of the mechanical path on the active control of noise transmission into an acoustic cavity.[16] Using a given configuration, they showed that the existence of the structural transmitting path presents formidable challenges to the control, in terms of both sensing arrangement and actuation mechanism. In fact, different transmitting paths (acoustic or structural) call for different control strategies. If the acoustic transmitting path is dominant, acoustic treatment or controlling the sound field inside the gap would be a natural choice, whereas when the structural transmitting path is dominant, effort might be put on reducing structural energy transmission. In a double-wall system, the energy transmission depends on many parameters such as the gap dimension, structural details and properties of the mechanical link. For a given configuration, unfortunately, unless a complete vibroacoustic analysis is performed, which is rather complicated and computationally demanding, there exists no simple rules to assess the relative importance of each transmitting path to further guide the decision-making process in terms of control.

In this paper we attempt to bring some answers to the above mentioned problems. The configuration under investigation is a mechanically linked double-wall structure, radiat-

[a]Author to whom correspondence should be addressed. Electronic mail: mmlcheng@polyu.edu.hk

 0001-4966/2005/117(5)/2742/10/$22.50

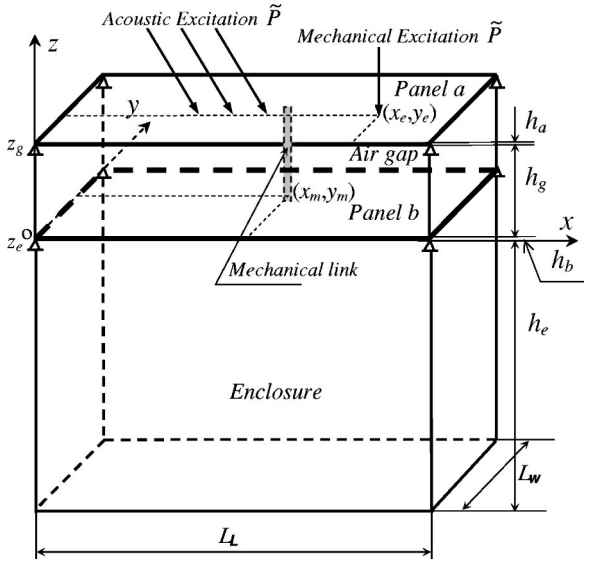

FIG. 1. Schematic representation of a mechanically linked double-wall structure.

ing sound into a rectangular acoustic enclosure. Theoretical development is first carried out, taking into account the full coupling between different components (two panels, mechanical links, the gap cavity and the enclosure). Numerical studies are then conducted to investigate the coupling characteristics of the system, providing general information on energy transmission between different components. A simple formula is derived to estimate the gap effect on the fundamental frequencies of the coupled system. Effects of the air gap and the mechanical link on energy transmission between the two walls, and the noise insulation properties are studied. It is shown that the effect of the gap can roughly be represented by an equivalent stiffness term, which is calculated using parameters related to the gap cavity. A simple criterion, based on the ratio between the aerostatic stiffness of the air gap and the stiffness of the mechanical link, is put forward to determine the dominant energy transmission path.

II. VIBROACOUSTIC MODELING

The structure under investigation, which comprises a double-wall structure connected to an acoustic enclosure and a mechanical link, is shown in Fig. 1. The double-wall structure is composed of two homogeneous and isotropic rectangular panels, which are simply supported along their boundaries and separated by an air gap cavity with a volume V_g. A mechanical link, located at (x_m,y_m), connects the two panels by its translational stiffness. The upper panel, called panel *a*, is subjected to external excitations; whereas the lower one, denoted as panel *b*, is coupled to the acoustic enclosure with a volume V_e. Apart from the surfaces occupied by the two panels, A_a and A_b, all other surrounding walls of both the air gap and the enclosure are acoustically rigid.

A brief description on the vibroacoustic modeling of the coupled system is presented. For the two panels, the equations of motion under an external excitation $\tilde{P}$ can be described as

$$D_a\nabla^4 w_a+\rho_a h_a\frac{\partial^2 w_a}{\partial t^2}=\tilde{P}-f_m\cdot\delta(x-x_m,y-y_m)-P_g(z_g=0), \quad (1)$$

for panel *a*, and

$$D_b\nabla^4 w_b+\rho_b h_b\frac{\partial^2 w_b}{\partial t^2}=f_m\cdot\delta(x-x_m,y-y_m)+P_g(z_g=h_g)-P_e(z_e=0), \quad (2)$$

for panel *b*. In the above equations, w_a, D_a, ρ_a and h_a are the transverse displacement (positive downwards), the flexible rigidity, the density and the thickness of panel *a*, respectively. Symbols with subscript *b* have the same meanings as defined above but applied to panel *b*. P_g and P_e are the acoustic pressures inside the air gap and the enclosure, respectively. $\tilde{P}$ can either be a point force or an acoustic pressure. In the former case, by neglecting the fluid loading on the emitter side of the system, a harmonic point force of amplitude F_0 applied at location (x_e,y_e) is assumed,

$$\tilde{P}(x,y,t)=F_0\delta(x-x_e,y-y_e)e^{i\omega t}, \quad (3a)$$

in which δ is the Dirac delta function. As to the latter, an oblique incident plane wave is assumed. In general, the total pressure acting on the panel can be decomposed into three parts, i.e., the incident pressure, the reflected pressure when the panel is assumed rigid and the radiated pressure due to the panel vibration. It is generally accepted that the radiated pressure is rather low compared to the other two components. Therefore, by neglecting the radiated pressure towards the outside and assuming equal magnitudes for the incident and reflected pressure waves, the excitation pressure on the panel is twice the magnitude of the incident wave, known as blocked pressure:[17]

$$\tilde{P}(x,y,t)=2P_0\exp(i\omega t-ik_0z\cos\phi-ik_0x\sin\phi\cos\theta-ik_0y\sin\phi\sin\theta), \quad (3b)$$

where P_0 is the amplitude of the incident pressure, and ϕ and θ are the elevation angle and azimuth angle, respectively. $k_0=\omega/c_0$ is the wave number with c_0 being the sound speed.

In Eqs. (1)–(2), f_m is the force produced by the mechanical link, which can be simulated by a spring with a stiffness K_m as

$$f_m=K_m[w_a(x_m,y_m)-w_b(x_m,y_m)]. \quad (4)$$

In light of modal superposition theory,[18] w_a and w_b can be decomposed over their respective mode shape functions $\varphi_{a,ij}(x,y)$ and $\varphi_{b,ij}(x,y)$ of panels *a* and *b* as

$$w_a(x,y,t)=\sum_i\sum_j\varphi_{a,ij}(x,y)q_{a,ij}(t), \quad (5a)$$

$$w_b(x,y,t)=\sum_i\sum_j\varphi_{b,ij}(x,y)q_{b,ij}(t), \quad (5b)$$

where $q_{a,ij}(t)$ and $q_{b,ij}(t)$ are the modal coordinates to be determined. Substituting Eq. (5) into Eqs. (1), (2), introduc-

ing viscous damping terms and applying the orthogonality properties of shape functions yield

$$\ddot{q}_{a,kl}(t)+2\zeta_{a,kl}\omega_{a,kl}\dot{q}_{a,kl}(t)+\omega_{a,kl}^2 q_{a,kl}(t)$$
$$=\frac{1}{m_{a,kl}}\left\{\tilde{P}\varphi_{a,kl}(x_e,y_e)-f_m\varphi_{a,kl}(x_m,y_m)-\int\int P_g\varphi_{a,kl}\,dx\,dy\right\}, \tag{6}$$

$$\ddot{q}_{b,kl}(t)+2\zeta_{b,kl}\omega_{b,kl}\dot{q}_{b,kl}(t)+\omega_{b,kl}^2 q_{b,kl}(t)$$
$$=\frac{1}{m_{b,kl}}\left\{f_m\varphi_{b,kl}(x_m,y_m)+\int\int (P_g-P_e)\times\varphi_{b,kl}\,dx\,dy\right\},\quad k=1,...,\mathsf{M};\quad l=1,...,\mathsf{N}, \tag{7}$$

where $\omega_{a,kl}$ (or $\omega_{b,kl}$) and $m_{a,kl}$ (or $m_{b,kl}$) are the klth natural angular frequency and the generalized mass of the klth mode of panel a (or b), respectively.

The acoustic pressure P_g inside the gap cavity is governed by the classical wave equation,

$$\nabla^2 P_g-\frac{1}{c_0^2}\frac{\partial^2 P_g}{\partial t^2}=0, \tag{8a}$$

with the constraint of the continuity of velocity on different parts of the cavity walls,

$$\frac{\partial P_g}{\partial \mathbf{n}}=\begin{cases}\rho\ddot{w}_a, & \text{on panel } a,\\ -\rho\ddot{w}_b, & \text{on panel } b,\\ 0, & \text{on the rigid wall,}\end{cases} \tag{8b}$$

where ρ is the equilibrium fluid density and $\mathbf{n}$ the normal direction towards the outside. In general, P_g can also be decomposed on the basis of acoustic mode shapes $\psi_{g,j}$ as

$$P_g=\sum_j \psi_{g,j}p_{g,j}(t), \tag{9a}$$

with

$$\nabla^2\psi_{g,j}=-\left(\frac{\omega_{g,j}}{c_0}\right)^2\psi_{g,j}, \tag{9b}$$

$$\frac{1}{V_g}\int_{V_g}\psi_{g,i}\psi_{g,j}\,dv=\begin{cases}0, & i\neq j,\\ m_{g,jj}, & i=j,\end{cases} \tag{9c}$$

where $p_{g,j}(t)$, $\omega_{g,j}$ and $m_{g,jj}$ stand for the jth modal pressure amplitude, angular frequency and the generalized mass of the gap cavity, respectively. The following Green's theorem[19] can then be used to transform the above wave equation into a set of ordinary differential equations:

$$\int_{V_g}(P_g\nabla^2\psi_g-\psi_g\nabla^2 P_g)dv=\int_{A_a}\left(P_g\frac{\partial\psi_g}{\partial\mathbf{n}}-\psi_g\frac{\partial P_g}{\partial\mathbf{n}}\right)ds. \tag{10}$$

Substituting Eq. (9) into (10) and introducing a modal loss factor $\zeta_{g,j}$ lead to the following set of acoustic equations for the gap cavity:

$$\ddot{p}_{g,j}(t)+2\zeta_{g,j}\omega_{g,j}\dot{p}_{g,j}(t)+\omega_{g,j}^2 p_{g,j}(t)$$
$$=\frac{\rho c_0^2}{m_{g,jj}V_g}\left[A_a\sum_k\sum_l L_{j,kl}^{ag}\ddot{q}_{a,kl}(t)-A_b\sum_k\sum_l L_{j,kl}^{bg}\ddot{q}_{b,kl}(t)\right],\quad j=1,...,n_g,$$
$$n_g=n_{gx}\times n_{gy}\times n_{gz}, \tag{11}$$

where (n_{gx},n_{gy},n_{gz}) are the numbers of modes used in modal expansions for the gap cavity. $L_{j,kl}^{ag}$ and $L_{j,kl}^{bg}$ are the modal coupling coefficients between the jth cavity mode of the gap cavity and the klth structural mode of panels a and b, respectively:

$$L_{j,kl}^{ag}=\frac{1}{A_a}\int_{A_a}\psi_{g,j}\varphi_{a,kl}\,ds,\quad L_{j,kl}^{bg}=\frac{1}{A_b}\int_{A_b}\psi_{g,j}\varphi_{b,kl}\,ds. \tag{12}$$

In the absence of mechanical links, the structural–acoustic coupling occurs in a very selective way due to the orthogonality of trigonometric functions involved in mode shape functions. For instance, any symmetric mode of the panel is decoupled to an acoustic mode as long as the latter is antisymmetrical in one of the two directions parallel to the panel surface.

Similarly, the acoustic pressure P_e inside the enclosure is expressed as

$$\ddot{p}_{e,j}(t)+2\zeta_{e,j}\omega_{e,j}\dot{p}_{e,j}(t)+\omega_{e,j}^2 p_{e,j}(t)$$
$$=\frac{\rho c_0^2 A_b}{m_{e,jj}V_e}\sum_k\sum_l L_{j,kl}^{be}\ddot{q}_{b,kl}(t),\quad j=1,...,n_e;$$
$$n_e=n_{ex}\times n_{ey}\times n_{ez}. \tag{13}$$

In Eq. (13), the quantities with the subscript "e" have the same meaning as those defined before but apply to the enclosure. In the case where the harmonic excitation is assumed,

$$q_{a,kl}(t)=a_{kl}e^{i\omega t},\quad q_{b,kl}(t)=b_{kl}e^{i\omega t},$$
$$p_{g,j}(t)=c_j e^{i\omega t},\quad p_{e,j}(t)=d_j e^{i\omega t}. \tag{14}$$

Equations (6), (7), (11), (13) can be combined in matrix form:

$$\begin{bmatrix}H_{11} & H_{12} & H_{13} & 0\\ H_{21} & H_{22} & H_{23} & H_{24}\\ H_{31} & H_{32} & H_{33} & 0\\ 0 & H_{42} & 0 & H_{44}\end{bmatrix}\begin{Bmatrix}A\\ B\\ C\\ D\end{Bmatrix}=\begin{Bmatrix}F_a\\ 0\\ 0\\ 0\end{Bmatrix}, \tag{15}$$

where $H_{11},\ldots,$ and H_{44} are coefficients calculated using expressions given in the Appendix. F_a is the generalized force applied to panel a. $A_{\mathsf{MN}\times 1}=\{a_{11},\ldots,a_{\mathsf{MN}}\}^T$, $B_{\mathsf{MN}\times 1}=\{b_{11},\ldots,b_{\mathsf{MN}}\}^T$, $C_{n_g\times 1}=\{c_1,\ldots,c_{n_g}\}^T$, $D_{n_e\times 1}=\{d_1,\ldots,d_{n_e}\}^T$.

Equation (15) describes the vibroacoustic behavior of the coupled system, which can be used to calculate various coefficients for constructing the displacement of each panel and the acoustic pressures inside the air gap and the enclo-

sure. It is evident that the formulation takes the full coupling between different components of the system into account, as reflected by the presence of terms $H_{12},\ldots,H_{42}$.

Two parameters, related to the vibration of the panels and the acoustic field, are defined as follows.[20]

(1) Averaged quadratic velocity $\langle V^2\rangle$,

$$\langle V^2\rangle = \begin{cases} \langle V^2\rangle_a = \dfrac{\omega^2}{2A_a}\displaystyle\int_{A_a} w_a w_a^*\, ds, & \text{for panel } a, \\ \langle V^2\rangle_b = \dfrac{\omega^2}{2A_b}\displaystyle\int_{A_b} w_b w_b^*\, ds, & \text{for panel } b, \end{cases} \tag{16}$$

where the asterisk denotes the complex conjugate of the quantity. In the following, $\langle V^2\rangle$ is expressed in dB referenced to $2.5\times10^{-15}\,\mathrm{m^2/s^2}$.

(2) Averaged sound pressure level L_p,

$$L_p = \begin{cases} L_{p,g} = 10\log(\langle P_g^2\rangle/P_{\mathrm{ref}}^2), & \text{for air gap}, \\ \langle P_g^2\rangle = \dfrac{1}{2V_g}\displaystyle\int_{V_g} P_g P_g^*\, dv, & \\ L_{p,e} = 10\log(\langle P_e^2\rangle/P_{\mathrm{ref}}^2), & \text{for enclosure}, \\ \langle P_e^2\rangle = \dfrac{1}{2V_e}\displaystyle\int_{V_e} P_e P_e^*\, dv, & \end{cases} \tag{17}$$

where $P_{\mathrm{ref}} = 20\ \mu\mathrm{Pa}$.

III. NUMERICAL RESULTS AND DISCUSSIONS

A double-wall structure with a dimension of $L_{\mathrm{L}}\times L_{\mathrm{W}}\times h_a = 0.5\times0.35\times0.002\ \mathrm{m}^3$ for the upper aluminum plate, *a*, and of $L_{\mathrm{L}}\times L_{\mathrm{W}}\times h_b = 0.5\times0.35\times0.003\ \mathrm{m}^3$ for the lower one, *b*, is used in numerical simulations. The depth of the enclosure is set as $h_e = 0.55$ m, while the depth of the air gap h_g varies to investigate the gap effect. The modal loss factors are assumed as 0.005 for the two panels and 0.001 for the gap cavity and the enclosure.

The number of modes used for both structural displacement and sound pressure decomposition is the main factor affecting the accuracy of the solution. In general, the accuracy can be satisfied by increasing the number of modes until convergence is achieved in the frequency range of interest. In the present case, a careful convergence study was carried out by increasing the number for each variable involved in the modal expansion series, leading to the following selection: (9,7,2) for the gap cavity, (9,7,8) for the enclosure and (10,10) for the two panels.

A. Fundamental frequencies of the coupled system

Prior to detailed analyses on energy transmission, a proper estimation of the aerostatic stiffness of the air gap is necessary. A good indication of the aerostatic stiffness of the air gap is the changes in the low-order natural frequencies of the coupled system due to the variation of h_g.

Upon assuming that only the mode (0,0,0) of the air gap affects the system, the first natural frequency of a cavity-backed panel (with a hard bottom) f_{coupled} can be estimated as[20]

$$f_{\mathrm{coupled}} = \left(f_{\mathrm{in\ vacuo}}^2 + \frac{1}{4\pi^2}\frac{\rho c_0^2 A_a^2 L_{0,s}^2}{m_s V_g} \right)^{1/2}, \tag{18}$$

where $f_{\mathrm{in\ vacuo}}$ is the fundamental frequency of the panel *in vacuo*, m_s is the generalized modal mass and $L_{0,s}$ the coupling coefficient between the *first panel mode* and the mode *(0,0,0) of the cavity*.

In the case of a double-wall structure, the stiffness of the air gap, seen by both panels, is frequency dependent. As far as low frequency modes are concerned, however, the effect of mode (0,0,0) is overwhelming over other modes. Using Eq. (18), an aerostatic stiffness term K_g can be defined as

$$K_g = \frac{\rho c_0^2 A_a^2 L_{0,s}^2}{V_g}. \tag{19}$$

Since the effect of the shallow gap on structural vibration surpasses that of the enclosure, a set of truncated equations can be obtained from Eq. (15) by neglecting terms related to the enclosure, while keeping those related to the first mode of each panel and mode (0,0,0) of the air gap. This operation leads to the following frequency equation:

$$\omega^4 - (\omega_a^2+\omega_b^2+\epsilon_a^2+\epsilon_b^2)\omega^2 + (\omega_a^2\omega_b^2+\epsilon_b^2\omega_a^2+\epsilon_a^2\omega_b^2) = 0, \tag{20}$$

with

$$\epsilon_a = \sqrt{\frac{K_g}{m_{a,11}}}, \quad \epsilon_b = \sqrt{\frac{K_g}{m_{b,11}}}, \tag{21}$$

where ω_a and ω_b are, respectively, the *in vacuo* fundamental angular frequencies of panels *a* and *b*; $m_{a,11}$ and $m_{b,11}$ are their corresponding generalized masses.

Solving Eq. (20) yields

$$\omega^2 = (\omega_a^2+\omega_b^2+\epsilon_a^2+\epsilon_b^2 \pm \sqrt{\epsilon_{ab}})/2, \tag{22}$$

where

$$\epsilon_{ab} = (\omega_a^2+\omega_b^2+\epsilon_a^2+\epsilon_b^2)^2 - 4(\omega_a^2\omega_b^2+\epsilon_b^2\omega_a^2+\epsilon_a^2\omega_b^2). \tag{23}$$

Thus, for the coupled system, the *first two* natural frequencies can be calculated by

$$f_{\mathrm{coupled}} = \left(\frac{f_a^2+f_b^2}{2} + \frac{1}{8\pi^2}\cdot(\epsilon_a^2+\epsilon_b^2 \pm \sqrt{\epsilon_{ab}}) \right)^{1/2}. \tag{24}$$

Equation (24) shows that f_{coupled} depend on both the frequencies of the fundamental mode of each panel and the aerostatic stiffness of the air gap. It can been seen from Eqs. (19), (21) and (24) that a decrease of h_g leads to an increase of ϵ_a and ϵ_b, and subsequently the f_{coupled}. Figure 2 compares the *first* f_{coupled} calculated by Eq. (24) with the result obtained by the full coupling analysis based on Eq. (15) in terms of f_{coupled}/f_a ($f_a = 59.7$ Hz) using different h_g/h_e. A good agreement between the two curves shows the validity of the formula given by Eq. (24). As a special case when panel *b* is immovable, it can be mathematically shown that Eq. (24) gives the same expression as Eq. (18), the validity of which is also shown in Fig. 2. In both cases, it can be seen that the derived formula gives a very good prediction on the changes in f_{coupled} caused by the air gap. A shallow gap increases

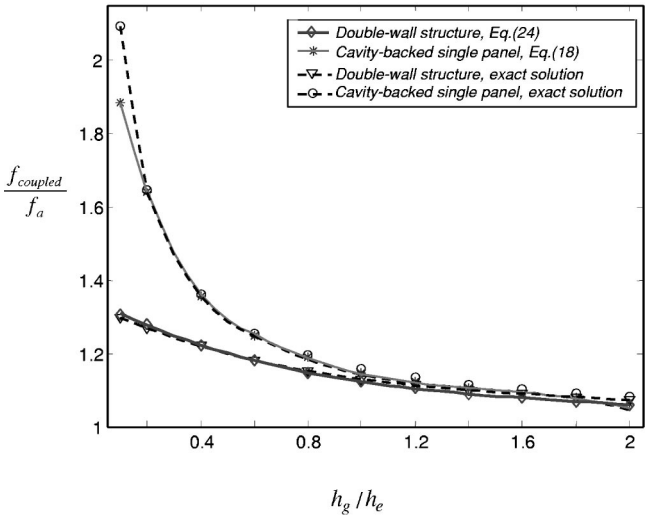

FIG. 2. Frequency variation of the *first* vibration mode of panel *a* with h_g/h_e varying from 0.05 to 2.

f_{coupled} to a lesser degree if both panels are flexible. This effect tends to be negligible when h_g becomes larger.

B. Mechanical excitation with subsections

1. General analysis

In this section, a harmonic exciting force with an amplitude of 1 N is applied to panel *a* at $(0.4L_{\text{L}},0.4L_{\text{W}})$. To gain basic understandings, a coupling analysis without mechanical links is first investigated. The depth of the air gap is set as $h_g=0.6h_e$. The natural frequencies of the coupled system, together with those of the corresponding uncoupled components (panels *a* and *b*, the air gap and the enclosure) are tabulated in Table I. A comparison between the two cases shows a significant alteration of the first two frequencies, dominated by panel *a* and *b*, respectively, in agreement with the results presented in Sec. III A. It should be pointed out that for the coupled system, the values of the natural frequencies are determined from the peak locations of the forced response curves, instead of solving the coupled eigenvalue problem. In order to identify the nature of a mode, the responses of each panel or the acoustic pressures of each cavity at the resonant frequency of the coupled system are calculated. Contributions of each subsystem can therefore be identified to determine the dominant component. The classification of different types of modes in a coupled system has been investigated previously.[21] For the sake of convenience, a mode is loosely labeled as ''mode dominated by one component'' to show the dominance of said component and the closeness of its natural frequency to its uncoupled counterpart.

As an example, the normal displacements of both panels at the first two resonant frequencies and the corresponding fluid velocities in the *z* direction in the gap cavity (contour) are illustrated in Fig. 3. It can be seen that the first mode (ω=67.3 Hz) is mainly dominated by panel *a* [Fig. 3(a)]; whereas the second one (ω=96.7 Hz) by panel *b* [Fig. 3(c)]. The two modes involve in-phase and out-of-phase motions of the two panels, respectively. The velocity contours given by Figs. 3(b) and 3(d) clearly show the phenomenon of air pumping (stiffness effect) due to the difference between the motions of the two panels.

Figures 4(a) and 4(b) show the spectra of the averaged quadratic velocity $\langle V^2\rangle$ of the two panels and the averaged sound pressure level L_p inside the air gap and the enclosure, respectively. Various peaks are marked with different sym-

TABLE I. Natural frequencies of the system in Hz ($h_g/h_e=0.6$).

Uncoupled case						
Mode\ Components	Panel *a*	Panel *b*	Mode\ Component	Air gap	Mode\ Component	Enclosure
(1,1)	59.7	89.6	(0,0,0)	0	(0,0,0)	0
(2,1)	118.6	177.9	(1,0,0)	340.0	(0,0,1)	309.1
(1,2)	179.9	269.9	(0,1,0)	485.7	(1,0,0)	340.0
(3,1)	216.8	325.2	(0,0,1)	515.2	(1,0,1)	459.5
(2,2)	238.8	358.3			(0,1,0)	485.7
(3,2)	337.0					
(4,1)	354.2					
(1,3)	380.3					
(2,3)	439.2					
(4,2)	474.5					
	Coupled case: Modes dominated by					
	Panel *a*	Panel *b*		Air gap		Enclosure
	67.3	96.7		0		0
	117.2	175.0		339.0		308.8
	178.5	266.8		486.8		341.4
	216.1	325.3				459.9
	237.5	356.5				486.8
	335.8					
	356.5					
	378.0					
	438.3					
	473.1					

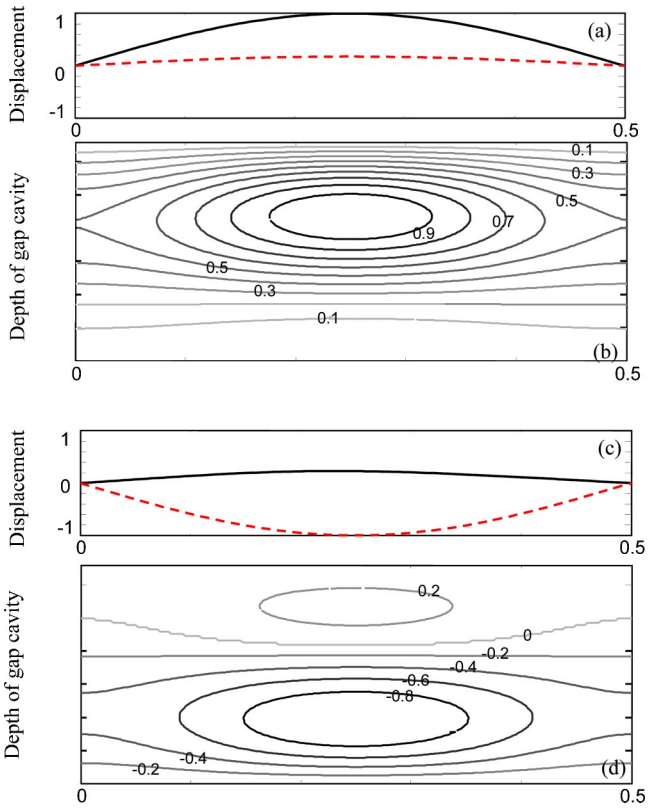

FIG. 3. Normal displacements of both panels at the first two resonant frequencies and the corresponding fluid velocities in the z direction at cross section $y=b_1/2$ in the air gap. (a) Displacements of two panels, $\omega=67.3$ Hz; (b) velocity distribution, $\omega=67.3$ Hz; (c) displacements of two panels, $\omega=96.7$ Hz; and (d) velocity distribution, $\omega=96.7$ Hz (a solid line for panel a and dashed for panel b).

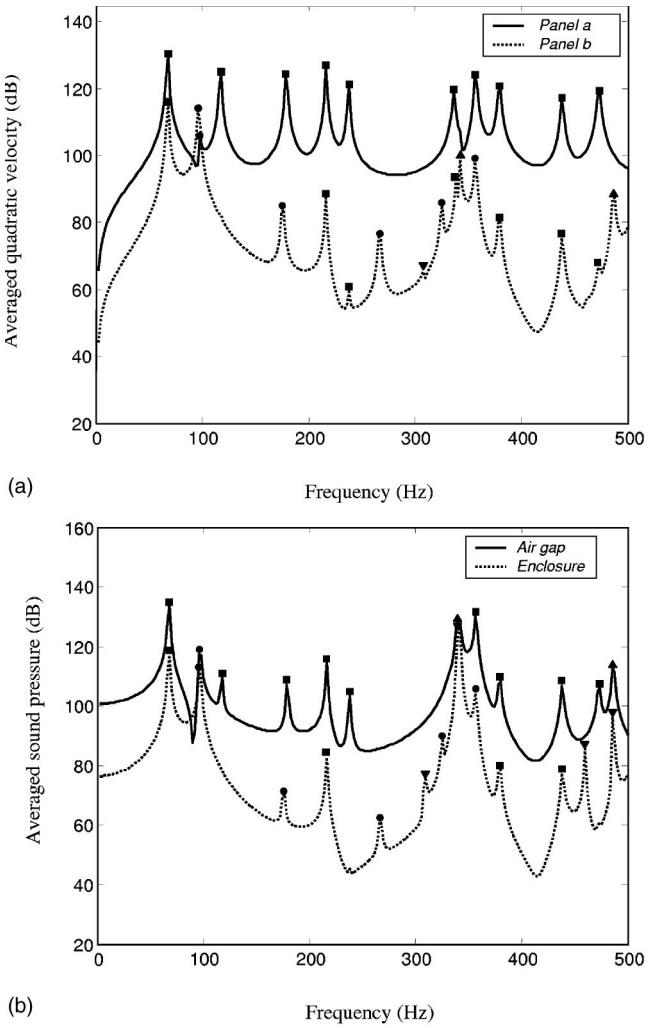

FIG. 4. (a) Averaged quadratic velocity $\langle V^2\rangle$ of panels a and b when $h_g/h_e=0.6$. ■: modes dominated by panel a; ●: modes dominated by panel b; ▲: modes dominated by the air gap; ▼: modes dominated by the enclosure. (b) Averaged sound pressure L_p inside the air gap and the enclosure when $h_g/h_e=0.6$.

bols so as to identify modes of a different nature. Figure 4(a) shows an obvious difference of around 30 dB in $\langle V^2\rangle$ between the two panels. Panel a exhibits resonances at frequencies close to its own natural frequencies. Via the air gap, the feedback effect of the panel b on a is relatively weak, since only the first mode of the panel b can be detected in $\langle V^2\rangle_a$. However, the forward energy transmission through the air gap (from a to b) is evident, because most of the resonance peaks dominated by panel a clearly appear in $\langle V^2\rangle_b$. Resonances of the air gap at 340 Hz (1,0,0) and 485.7 Hz (0,1,0) create a negligible effect on panel a, but an obvious effect on panel b. All peaks identified in $\langle V^2\rangle_a$ induce high sound pressure in the air gap, as shown in Fig. 4(b). In addition, two resonances of the air gap give raise to high acoustic energy concentration. Comparing the sound pressure levels inside the two cavities, it can be seen that the sound transmission is particularly high at the first two resonances, related to panels a and b, respectively, and also at modes (1,0,0) and (0,1,0), where both the air gap and the enclosure undergo resonances. Generally speaking, the results based on the present configuration without a mechanical link seem to imply a clear forward transmission path (panel a—air gap, panel b—enclosure) with a relatively small feedback effect.

2. Effect of the depth hg

In order to reveal the effect of the depth of the air gap h_g, the case when $h_g/h_e=0.2$ is studied and the spectra of $\langle V^2\rangle$ and L_p are plotted in Fig. 5, together with their counterparts when $h_g/h_e=0.6$ (already shown in Fig. 4) for comparison purposes. It can be seen from Fig. 5(a) that a decrease in h_g leads to an increase in the aerostatic stiffness of the air gap, consequently resulting in an obvious increase in the *first two* resonance frequencies dominated by panels a and b, respectively. For the same token, the feedback effect of the acoustic mode (1,0,0) of the air gap at 340 Hz creates an obvious peak in $\langle V^2\rangle_a$ [denoted by a "▲" in Fig. 5(a)], implying a more significant coupling and a stronger reverberation of energy when the double-wall structure has a shallow gap. Apart from these particular frequencies, the overall level of $\langle V^2\rangle_a$ is basically not affected. Subsequent energy transmissions, however, be it for $\langle V^2\rangle_b$ in Fig. 5(a), or $L_{p,g}$ and $L_{p,e}$ in Fig. 5(b), are all systematically increased to almost the same extent due to the decrease of h_g.

3. Effect of the mechanical link

A mechanical link, modeled as a punctual translational spring with a stiffness of $K_m=10^6$ N/m is assumed to connect the two panels at $(0.6L_L,0.6L_W)$. The spectra $\langle V^2\rangle$ and

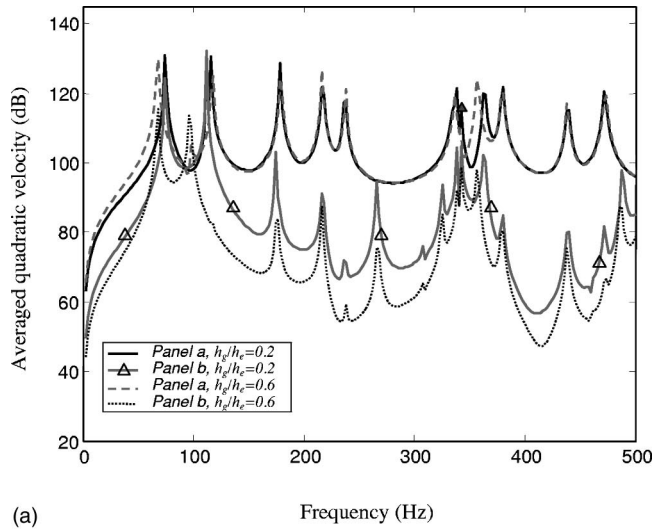

FIG. 5. (a) Averaged quadratic velocity $\langle V^2 \rangle$ of panels a and b when $h_g/h_e=0.2$ and 0.6. (b) Averaged sound pressure L_p inside the air gap and the enclosure when $h_g/h_e=0.2$ and 0.6.

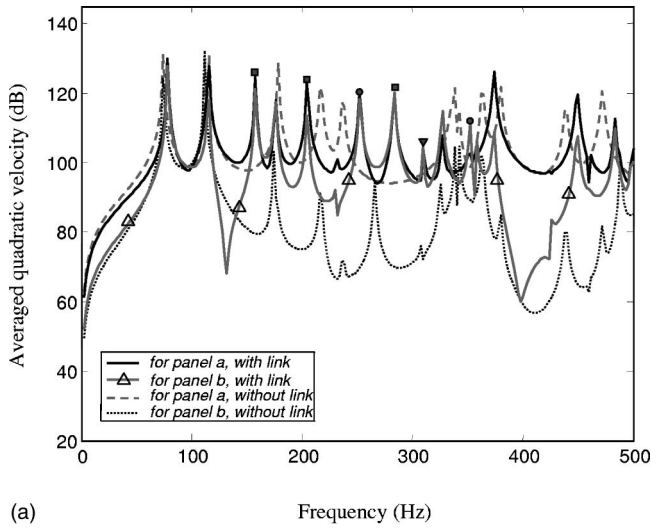

FIG. 6. (a) Averaged quadratic velocity $\langle V^2 \rangle$ of panels a and b of a double-wall structure with ($K_m=10^6$ N/m) and without ($K_m=0$) a link when $h_g/h_e=0.2$. (b) Averaged sound pressure level L_p inside the gap and the enclosure with ($K_m=10^6$ N/m) and without ($K_m=0$) a link when $h_g/h_e=0.2$.

L_p when $h_g/h_e=0.2$ with and without the link are plotted in Figs. 6(a) and 6(b), respectively. It can be seen that, compared with the case without a mechanical link, the transmission of vibration energy from panel a to b is significantly increased [Fig. 6(a)], resulting in an increase in L_p inside both cavities [Fig. 6(b)]. Although the vibration level of panel a remains more or less the same, resonance peaks are evidently altered. In addition, resonance peaks dominated by panel b can also be clearly identified in $\langle V^2 \rangle_a$ as well as in $L_{p,g}$ and $L_{p,e}$. These results indicate a strong coupling between the two panels and a more significant energy transmission due to the introduction of a mechanical link, which is quite understandable.

4. Comparison between gap effect and mechanical effect on energy transmission

Previous results show that energy can be transmitted either through the acoustic path, especially with a shallow air gap, or through the structural path with a mechanical link, which are reflected by the parameters h_g and K_m. In this section we aim at developing a criterion to predict the dominant transmission path in the presence of a mechanical link.

Based on the fact that the area under the spectrum of the averaged quadratic velocity $\langle V^2 \rangle$ can roughly represent the energy level within the analyzed frequency band, a global index characterizing energy transmission between the two panels can then be defined as

$$\gamma_{\mathrm{pl}}=E_{\mathrm{pl},b}/E_{\mathrm{pl},a}, \tag{25a}$$

with

$$E_{\mathrm{pl},b}=\frac{1}{2}\rho_b h_b A_b \overline{\langle V^2 \rangle}_b, \quad E_{\mathrm{pl},a}=\frac{1}{2}\rho_a h_a A_a \overline{\langle V^2 \rangle}_a, \tag{25b}$$

in which $\overline{\langle V^2 \rangle}_b$ and $\overline{\langle V^2 \rangle}_b$ are the areas under the spectra $\langle V^2 \rangle_b$ and $\langle V^2 \rangle_a$, respectively.

Figure 7(a) illustrates the tendency plot of γ_{pl} with different depth ratios h_g/h_e and stiffness K_m of the mechanical link. γ_{pl} decreases either with a decreasing K_m or an increasing h_g/h_e, in agreement with observations made in Figs.

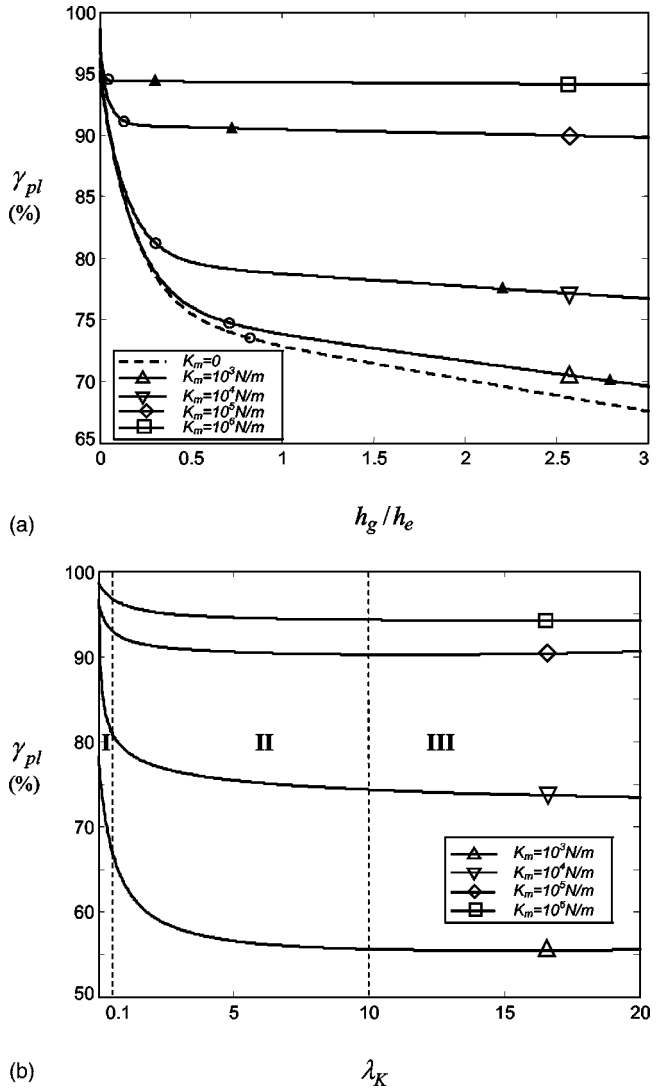

FIG. 7. Tendency plot of γ_{pl} showing the energy transmission between two walls: (a) with respect to h_g/h_e; (b) with respect to λ_K.

5(a) and 6(a). Given a K_m, γ_{pl} drops rapidly with the increase of h_g/h_e, then smoothly bends before reaching a plateau. This tendency is most obvious when K_m becomes relatively large. Obviously, the energy transmission undergoes *three* different zones. In the first fast dropping zone (before the symbol "○" in the curve), where the gap between two walls is shallow, γ_{pl} is very sensitive to h_g/h_e, meaning that a slight change in h_g has a significant impact on energy transmission between the two panels. Therefore, most energy will be transmitted from panel *a* to *b* through the air gap. The second zone is characterized by a smooth drop of γ_{pl} (ended by a "▲" in the curve), within which the gap effect on energy transmission is weakened and the air gap can be regarded as a soft spring. Energy is then transmitted simultaneously through the link and the air gap. In the plateau zone, γ_{pl} is insensitive to h_g/h_e, implying that most energy is transmitted through the mechanical link rather than the air gap. The separating points between different zones apparently depend on the value of K_m, which a stiff mechanical link reduces the *first two* zones.

The prediction of these three zones is helpful for determining the most significant energy transmitting path. To this end, a new parameter, defined as the ratio between the stiffness K_m of mechanical link and the aerostatic stiffness K_g of the air gap, is used to generalize the aforementioned phenomena:

$$\lambda_K = \frac{K_m}{K_g}. \tag{26}$$

Using this normalized parameter λ_K, the same set of results used in Fig. 7(a) is plotted in Fig. 7(b), which shows a systematic demarcation of the three different zones, irrespective of individual values of K_m and h_g/h_e. Zone I is roughly delimited by $\lambda_K < 0.1$, in which the acoustic transmitting path is dominant; zone II is confined to $0.1 < \lambda_K < 10$, within which both acoustic and structural transmitting paths play important roles in energy transmission; and zone III covers the region $\lambda_K > 10$, in which energy transmission is mainly due to the structural path. Although the demarcation lines between different zones are very vague, the use of λ_K indeed facilitates the prediction of the dominant transmitting path, since the calculation of λ_K only uses the physical and geometrical parameters related to the mechanical link and the air gap.

C. Acoustic excitation

Different energy transmission paths between two walls certainly affect the noise isolation properties of the double-wall structure. This can be examined by investigating the noise peduction (NR) index when the panel *a* is subjected to an oblique incident plane wave. A NR index is defined as the difference between the outer surface-pressure level $L_{p,\mathrm{out}}$ and averaged inner enclosure-pressure $L_{p,e}$ as

$$\gamma_{NR} = L_{p,\mathrm{out}} - L_{p,e}, \tag{27a}$$

$$L_{p,\mathrm{out}} = 10\log(\langle P_{\mathrm{out}}^2\rangle / P_{\mathrm{ref}}^2), \tag{27b}$$

where $\langle P_{out}^2\rangle$ is the mean-square pressure averaged over the outside panel surface, i.e.,

$$\langle P_{\mathrm{out}}^2\rangle = \frac{1}{2A_a}\int_{A_a} P_{\mathrm{out}} P_{\mathrm{out}}^* \, ds. \tag{27c}$$

It should be pointed out that the above definition is different from the conventional NR in that the receiving side of the sound is an enclosure. As a result, the dynamic behavior of the enclosure has an influence on the resulting NR.

Figure 8(a) shows γ_{NR} when $h_g/h_e = 0.2$, for three cases: (1) $K_m = 0$ (without a link); (2) $K_m = 10^3$ N/m; and (3) $K_m = 10^6$ N/m. The excitation is an oblique plane wave with $P_0 = 1$ Pa, $\theta = 60°$ and $\phi = 30°$. All three cases exhibit a similar tendency when frequencies vary, i.e., poor insulation at low frequencies, especially around the *first two* resonances of the double-wall structure, with an obvious increase at higher frequencies. Comparing different cases shows very little difference between $K_m = 10^3$ N/m and $K_m = 0$ cases, meaning a negligible effect of K_m on NR for a soft link. With $K_m = 10^3$ N/m, the corresponding $\lambda_K = 0.03 < 0.1$ ($K_g = 3.625 \times 10^4$ N/m), which is indeed inside zone I, where acoustic transmitting path proves to be dominate. The increase in K_m from 10^3 N/m to 10^6 N/m pushes the case into zone III (λ_K

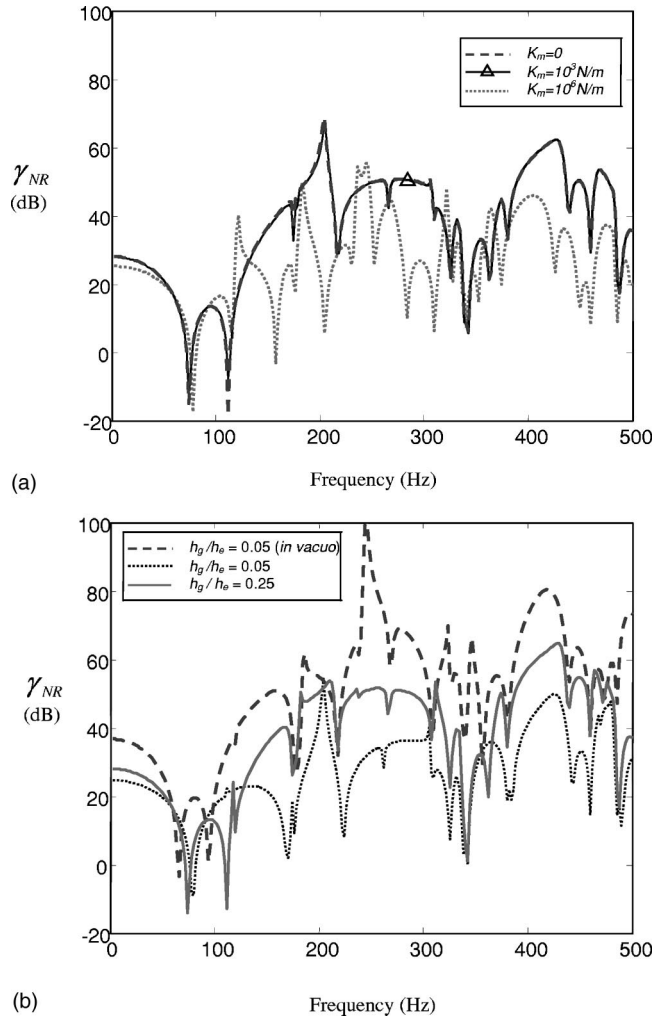

FIG. 8. Noise reduction index γ_{NR} of the double-wall structure. (a) Effect of the mechanical link; (b) effect of the depth of the gap.

$=28>10$), as evidenced by a clear decrease in γ_{NR} at frequencies above the *first two* resonances, implying a significant energy transmission through the structural path.

By keeping $K_m=10^4$ N/m, Fig. 8(b) shows the variation of γ_{NR} with two different gap depths: (1) $h_g/h_e=0.05$ (*in vacuo*, $\lambda_K=0.07$); (2) $h_g/h_e=0.05$; and (3) $h_g/h_e=0.25$ ($\lambda_K=0.34$). The difference in γ_{NR} between case (1) and case (2) shows a very significant energy transmission through the acoustic path. Increasing the depth of the air gap to $h_g/h_e=0.25$ approaches the γ_{NR} curve to that of case (1), implying a weakened acoustic transmitting path. If an even larger h_g/h_e is used (not shown), the γ_{NR} curve will converge to the *in vacuo* one, that is, a total energy transmission through the structural path.

As a final remark, the observed phenomena and the established criterion would also be useful in the modeling of the double-wall system. Most of the practical double-wall structures have closely spaced panels, which most likely fall into zones I and II. Such structures require the inclusion of the air gap into the modeling. An exception occurs when the two panels are widely separated and connected by very stiff mechanical joints (zone III). In such cases, the air gap between the panels can be ignored to simplify the modeling process.

IV. CONCLUSIONS

Based on a fully coupled vibroacoustic model, in the present paper we focus on the effect of the air gap and mechanical links on the energy transmission and noise insulation properties of a double-wall structure coupled to an acoustic enclosure. Results lead to the following conclusions.

(1) The existence of the mechanical link enhances the coupling between the two panels. As a result, the forward transmission path, the feedback effect and the reverberation of vibration energy between the two panels intensify.
(2) The depth of the air gap has significant effects on both the vibration of panels and the energy transmission. The shallow gap has a remarkable added-stiffness effect on the panels and increases the forward energy transmission. A simple formula is proposed to estimate the coupled fundamental frequencies of the double-wall structure without a mechanical link.
(3) In the presence of mechanical links, energy can be transmitted via both the acoustic path (through the air gap) and the structural path (through mechanical links). The stiffness of the mechanical link and the aerostatic stiffness of the air gap are shown to be two governing parameters. The latter can be roughly estimated using the definition given in the paper, which is based on the coupling between the first structural mode and the fundamental mode of the air gap. The ratio between the two stiffness terms forms a parameter λ_K, which can be used to identify the most dominant transmitting path in a given configuration. Numerical results reveal three different zones, which involve different transmission mechanisms. When λ_K is very small, e.g., $\lambda_K<0.1$, corresponding to a soft mechanical link or a shallow gap case, energy goes mainly through the air gap to the system. On the contrary, when λ_K is very large, e.g., $\lambda_K>10$, the mechanical link will be the main media for energy transmission. In the intermediate zone, both the air gap and the mechanical link are responsible for transmission.

It should be mentioned that the proposed demarcation values of λ_K, which are used to separate different zones, should be regarded as indicative values with a certain margin. The criterion put forward in the present study, in its simple form, provides a practical means to estimate the main energy transmission path without performing a complex vibroacoustic analysis. This information is believed to be useful for providing guide on the design of control systems.

ACKNOWLEDGMENTS

The authors would like to thank the Research Committee of The Hong Kong Polytechnic University and the Research Grants Council of HKSAR for the financial support

for this project. They are grateful to Professor J. Pan and Dr. C. Bao from University of Western Australia, for providing data used in model validation.

APPENDIX: CALCULATION OF H_{11},..., AND H_{44}

$$H_{11}=M_a+K_m\Phi_a^T(x_m,y_m)\Phi_a(x_m,y_m),$$

$$M_a=\begin{bmatrix}\ddots & & \\ & m_{a,ij}(\omega_{a,ij}^2+2i\zeta_{a,ij}\omega_{a,ij}\omega-\omega^2) & \\ & & \ddots\end{bmatrix}_{\mathrm{MN}\times\mathrm{MN}},$$

$$\Phi_a(x_m,y_m)=\lfloor\varphi_{a,11}(x_m,y_m),\varphi_{a,12}(x_m,y_m),\ldots,\varphi_{a,\mathrm{MN}}(x_m,y_m)\rfloor,$$

$$H_{12}=-K_m\Phi_a^T(x_m,y_m)\Phi_b(x_m,y_m),\quad H_{21}=H_{12}^T,$$

$$H_{22}=M_b+K_m\Phi_b^T(x_m,y_m)\Phi_b(x_m,y_m),$$

$$M_b=\begin{bmatrix}\ddots & & \\ & m_{b,ij}(\omega_{b,ij}^2+2i\zeta_{b,ij}\omega_{b,ij}\omega-\omega^2) & \\ & & \ddots\end{bmatrix}_{\mathrm{MN}\times\mathrm{MN}},$$

$$H_{13}^T=A_a\begin{bmatrix}L_{1,11}^{ag} & \cdots & L_{1,\mathrm{MN}}^{ag}\\ \cdots & \cdots & \cdots\\ L_{n_g,11}^{ag} & \cdots & L_{n_g,\mathrm{MN}}^{ag}\end{bmatrix},$$

$$H_{23}^T=-A_b\begin{bmatrix}L_{1,11}^{bg} & \cdots & L_{1,\mathrm{MN}}^{bg}\\ \cdots & \cdots & \cdots\\ L_{n_g,11}^{bg} & \cdots & L_{n_g,\mathrm{MN}}^{bg}\end{bmatrix},$$

$$H_{24}^T=A_b\begin{bmatrix}L_{1,11}^{be} & \cdots & L_{1,\mathrm{MN}}^{be}\\ \cdots & \cdots & \cdots\\ L_{n_e,11}^{be} & \cdots & L_{n_e,\mathrm{MN}}^{be}\end{bmatrix},$$

$$H_{31}=\frac{\rho c_0^2A_a\omega^2}{V_g}\begin{bmatrix}\frac{1}{m_{g,11}}[L_{1,11}^{ag}\ \cdots\ L_{1,\mathrm{MN}}^{ag}]\\ \cdots\\ \frac{1}{m_{g,n_gn_g}}[L_{n_g,11}^{ag}\ \cdots\ L_{n_g,\mathrm{MN}}^{ag}]\end{bmatrix},$$

$$H_{32}=-\frac{\rho c_0^2A_b\omega^2}{V_g}\begin{bmatrix}\frac{1}{m_{g,11}}[L_{1,11}^{bg}\ \cdots\ L_{1,\mathrm{MN}}^{bg}]\\ \cdots\\ \frac{1}{m_{g,n_gn_g}}[L_{n_g,11}^{bg}\ \cdots\ L_{n_g,\mathrm{MN}}^{bg}]\end{bmatrix},$$

$$H_{33}=\begin{bmatrix}\ddots & & \\ & -\omega^2+2i\zeta_{g,j}\omega_{g,j}\omega+\omega_{g,j}^2 & \\ & & \ddots\end{bmatrix}_{n_g\times n_g},$$

$$H_{42}=\frac{\rho c_0^2A_b\omega^2}{V_e}\begin{bmatrix}\frac{1}{m_{e,11}}[L_{1,11}^{be}\ \cdots\ L_{1,\mathrm{MN}}^{be}]\\ \cdots\\ \frac{1}{m_{e,n_en_e}}[L_{n_e,11}^{be}\ \cdots\ L_{n_e,\mathrm{MN}}^{be}]\end{bmatrix},$$

$$H_{44}=\begin{bmatrix}\ddots & & \\ & -\omega^2+2i\zeta_{e,j}\omega_{e,j}\omega+\omega_{e,j}^2 & \\ & & \ddots\end{bmatrix}_{n_e\times n_e}.$$

[1] A. London, "Transmission of reverberant sound through double wall," J. Acoust. Soc. Am. **22**, 270–279 (1950).
[2] L. L. Beranek, *Noise Reduction* (McGraw-Hill, New York, 1960).
[3] A. J. Price and M. J. Crocker, "Sound transmission through double panels using statistical energy analysis," J. Acoust. Soc. Am. **47**, 683–693 (1970).
[4] J. A. Steel and R. J. M. Craik, "Statistical energy analysis of structure-borne sound transmission by finite element methods," J. Sound Vib. **178**, 553–561 (1994).
[5] F. C. Sgard, N. Atalla, and J. Nicolas, "A numerical model for the low frequency diffuse field sound transmission loss of double-wall sound barriers with elastic porous linings," J. Acoust. Soc. Am. **108**, 2865–2872 (2000).
[6] H. Iwashige and M. Ohta, "A practical method of estimating sound-transmission loss of double walls—a proposal and its application to the popular case of light panels and air gap," Acustica **48**, 97–101 (1981).
[7] J. M. P. Antonio, A. Tadeu, and L. Godinho, "Analytical evaluation of the acoustic insulation provided by double infinite walls," J. Sound Vib. **263**, 113–129 (2003).
[8] L. Cremer and M. Heckl, *Structure-Borne Sound: Structural Vibrations and Sound Radiation at Audio Frequencies* (Springer-Verlag, Berlin, 1988).
[9] F. W. Grosveld and K. P. Shepherd, "Active sound-attenuation across a double-wall structure," J. Aircr. **31**, 223–227 (1994).
[10] P. Sas, C. Bao, F. Augusztinovisz, and W. Desmet, "Active control of sound transmission through a double-panel partition," J. Sound Vib. **180**, 609–625 (1995).
[11] C. Bao and J. Pan, "Experimental study of different approaches for active control of sound transmission through double walls," J. Acoust. Soc. Am. **102**, 1664–1670 (1997).
[12] C. Y. Wang and R. Vaicaitis, "Active control of vibrations and noise of double wall cylindrical shells," J. Sound Vib. **216**, 865–888 (1998).
[13] J. Pan and C. Bao, "Analytical study of different approaches for active control of sound transmission through double walls," J. Acoust. Soc. Am. **103**, 1916–1922 (1998).
[14] P. Gardonio and S. J. Elliott, "Active control of structure-borne and airborne sound transmission through double panel," J. Aircr. **36**, 1023–1032 (1999).
[15] H. Bouhioui, "Vibroacoustic study of a double glazing system (in French)," Université de Technologie de Compiègne, Compiègne, Ph.D. thesis, 1993.
[16] C. Bao and J. Pan, "Active acoustic control of noise transmission through double walls: Effect of mechanical paths," J. Sound Vib. **215**, 395–398 (1998).
[17] J. P. Carneal and C. R. Fuller, "An analytical and experimental investigation of active structural acoustic control of noise transmission through double panel systems," J. Sound Vib. **272**, 749–771 (2004).
[18] A. W. Leissa, *Vibration of Plates* (published for the Acoustical Society of America through the American Institute of Physics, Woodbury, NY, 1993).
[19] E. H. Dowell, G. F. Gorman, and D. A. Smith, "Acoustoelasticity: general theory, acoustic natural modes and forced response to sinusoidal excitation, including comparisons with experiment," J. Sound Vib. **52**, 519–541 (1977).
[20] L. Cheng and J. Nicolas, "Radiation of sound into a cylindrical enclosure from a point-driven end plate with general boundary conditions," J. Acoust. Soc. Am. **91**, 1504–1513 (1992).
[21] L. Cheng, "Fluid-structural coupling of a plate-ended cylindrical shell: vibration and internal sound field," J. Sound Vib. **174**, 641–654 (1994).